Light Scattering Cross Section of Hydrophilic and Hydrophobic Silica Aggregates

Frédéric Gruy, Michel Cournil

HAL Id: hal-00125359
https://hal.archives-ouvertes.fr/hal-00125359

Light Scattering Cross Section of Hydrophilic and Hydrophobic Silica Aggregates

F. GRUY*
M. COURNIL

Dept SPIN-LPMG UMR CNRS 5148
Ecole des Mines de Saint-Etienne,
158 Cours Fauriel, 42023 Saint-Etienne, France

* gruy@emse.fr

Abstract

The aggregation dynamics of solid particles in liquid media is currently followed by optical based particle sizing methods. Because it can be used *in situ* and applied to a wide particle size range, turbidimetry is acknowledged as one of the best methods for this characterization. Although much work has been done about aggregation, some aspects are less known and require additional experimental and theoretical research. This is particularly the case of aggregation of hydrophobic particles. Corresponding aggregates are 3-phase objects (solid-liquid-gas) the morphology and optical properties of which are not known. Present work rests on the turbidimetric study of hydrophilic and hydrophobic silica samples in stirred aqueous solutions. Modelling involves different aspects: aggregate morphology, aggregate optical properties, and aggregation dynamics. This paper particularly emphasizes the second one. Fractal-like models are proved to be representative of the aggregate morphology even at small size. Light scattering cross-section of the aggregates is calculated from their averaged projected area; effective refractive index is proved to be a good parameter for modelling their optical properties both for hydrophilic and hydrophobic aggregates. Classical models of porous aggregate formation (Kusters theory) are used for describing the aggregation dynamics.

Keywords : Light scattering ; aggregates ; hydrophilic ; hydrophobic ; silica.

Introduction

Aggregation of hydrophilic particles in stirred liquid media can be considered as a relatively well understood process in spite of the variety and complexity of its aspects: physico-chemical, hydrodynamic, morphological (Elimelech et al., 1995). On the contrary, aggregation of hydrophobic particles in aqueous media or more generally solid particles in non wetting media is less known, at least on certain aspects, particularly the aggregate structure and properties.

Experimental works have confirmed the existence of strong long range (20-200 nm) attractive forces between hydrophobic surfaces in water (Yushchenko et al., 1983; Parker et al., 1994). This hydrophobic interaction was quantified from direct force measurements and proved to be, in most cases, much larger than the van der Waals forces. Previous experimental results have given rise to intensive theoretical work about the origins of the hydrophobic interaction. Several interpretations have been explored in some details (Attard, 2003). It seems that the most likely explanation focuses upon the bridging of nanobubbles which are present on the hydrophobic surface. The existence of these bubbles was first deduced from force measurements and then confirmed by direct observations (Parker et al., 1994; Yabukov et al., 2000; Attard, 2003). Although experimental evidence and thermodynamic interpretation conclusively prove that gas bridging from pre-existing nanobubbles is of major importance in hydrophobic aggregation, some theoretical aspects are less understood. In particular, volume fraction and spatial repartition of gas in hydrophobic aggregates are not known.

Here a few results are presented from an experimental study of aggregation of two silica samples coming from the same lot: the original sample is naturally hydrophilic; the other has been made hydrophobic by surface chemical processing. Aggregation process is followed by

in situ turbidimetry, the interpretation of which requires knowledge of the light scattering cross section of aggregates.

Experimental Methodology

Materials and methods

Original solid samples consist of monodisperse silica spheres (0.5 µm in diameter, *Geltech Inc* product code: S0501). They are highly insoluble in water and can be made hydrophobic by superficial grafting of carbon chains. The grafting procedure consists first of an hydroxylation process which produces highly reactive silanol (-SiOH) groups, then of a wetting step with a N,N dimethyloctadecylaminosilane solution which produces the surface silanisation reaction, i.e. the grafting of a carbon chain via a strong Si-O-Si bond. The contact angle on this processed surface is 125° in pure water. Both silica particles, processed or unprocessed, have a zero point charge pH of 3.2 (Cugniet, 2003; Gruy et al., 2004).

The reactor is a double jacketed 4-baffled 1.45 L vessel. It is provided with a watertight cover so that it can be completely filled with liquid, avoiding in this the presence of a free interface which could entrap hydrophobic particles. Turbulent agitation is ensured by a four bladed 45° teflon impeller. Temperature is kept constant at 25.0°C. Each aggregation experiment consists of the following steps: preliminary dispersion by ultrasonics of 0.246 g of solid sample in an ethanol-rich small volume; filling-up of the reactor with water; injection of the silica suspension and destabilization by nitric acid addition (pH 2 to 4). Aggregation immediately starts and can be followed by turbidimetry.

Over the last ten years, we have developed several optical devices to determine in situ the particle size distribution (PSD) or the moments of particulate systems. For diluted

suspensions (solid volume fraction $\phi < 10^{-4}$), an optical sensor based on spectral turbidimetry principles can be used to determine the PSD of suspensions composed of submicronic and micronic particles (Crawley et al., 1997). The turbidity probe is vertically located at the two-thirds of the vessel radius halfway between two baffles, and mounted at third liquid height above the bottom of the tank. Light emitted by a Xenon UV light source is led by fibre optics to the probe window. The emerging light beam is collimated by a lens. When crossing the 1 cm optical path, light is scattered by the different particles and aggregates. Emerging light is collected by the same system (similar lens and fibre optics) and led to a commercial spectrophotometer which finally delivers the turbidity spectrum in the wavelength range [350 nm-800 nm]. Turbidity τ which expresses the extinction due to scattering by particles is defined by the relation:

$$\tau(\lambda_0) = \frac{1}{L_{opt}} \ln\left(\frac{I_0(\lambda_0)}{I(\lambda_0)} \right) \tag{1}$$

in which λ_0 is the wavelength, $I_0(\lambda_0)$ the intensity of the incident beam and $I(\lambda_0)$ the intensity of the transmitted beam after an optical path of length L_{opt}.

Principle of exploitation of the experimental data

In situ turbidimetry has been successfully applied by the authors to several systems in order to determine their aggregation dynamics. Details can be found in Cugniet (2003) and Saint-Raymond et al. (1998).

For a polydisperse population of particles, turbidity contains the contribution of each class of aggregate:

$$\tau(\lambda_0) = \sum_{i=1}^{N} C_{ext,i} N_i \tag{2}$$

where N_i is the number concentration of aggregates consisting of i primary particles. Particle extinction section $C_{ext,i}$ is derived from the Mie theory (van de Hulst, 1957); $C_{ext,i}$ depends on the particle diameter, on the refractive index ratio and on the wavelength. Its calculation is relatively easy for spherical, compact, or large particles. However, it is much more intricate for small, non compact aggregates. From equation (2) it can be seen that variations in the different aggregate concentrations N_i result in turbidity variation, thus the interest of turbidimetry to follow the aggregation process. When aggregation takes place in a liquid suspension, turbidity either increases or decreases versus time (Saint-Raymond et al., 1998; Gruy et al., 2004). From a general point of view, decreasing or increasing trend is determined both by the primary particle size and the refractive index ratio between the liquid phase and the aggregates. In both cases, amplitude of turbidity variation indicates the global extent of the whole process. Initial slope is proportional to the aggregation rate whereas non-zero height of the final plateau reveals the existence of aggregate maximum size possibly due to fragmentation.

Experimental results

Figures 1 and 2 represent respectively turbidity change with time for hydrophilic and hydrophobic silica ($\lambda = 550$ nm) in ethanol (3.45 %)-water (96.55 %) mixture. This composition corresponds to the smallest ethanol quantity leading to a high dispersion of hydrophobic silica suspension during sonication. Effect of the stirring rate on turbidity

variation with time has been examined in both cases. Relatively simple calculation using Mie theory (van de Hulst, 1957) shows that, for the present initial radius and refractive index values, turbidity should increase at least initially when aggregation proceeds. This is observed for the unprocessed particles. The opposite trend which is noted for hydrophobic silica can be explained by a decrease in the aggregate refractive index and a change in the index contrast between the liquid phase and the aggregate. Precisely, presence of gas (air or vapour) in an aggregate may considerably change this contrast and be responsible for the behaviour modification we noted. Referring to the usual models of hydrophobic interaction (Attard, 2003), this is a strong indication for the presence of gas bridges between the particles. Another confirmation can be found in the final value of the turbidity (Figures 1 and 2) which is very low in the case of hydrophobic particles and consistent with the formation of few large aggregates. In the case of unprocessed particles, the relatively high level of final turbidity indicates the presence of numerous small aggregates. The hydrophobic aggregates are apparently much less or even not at all sensitive to fragmentation in the same hydrodynamic conditions. This behaviour is as well consistent with the presence of gas bridges between the particles which strongly strengthen the aggregates.
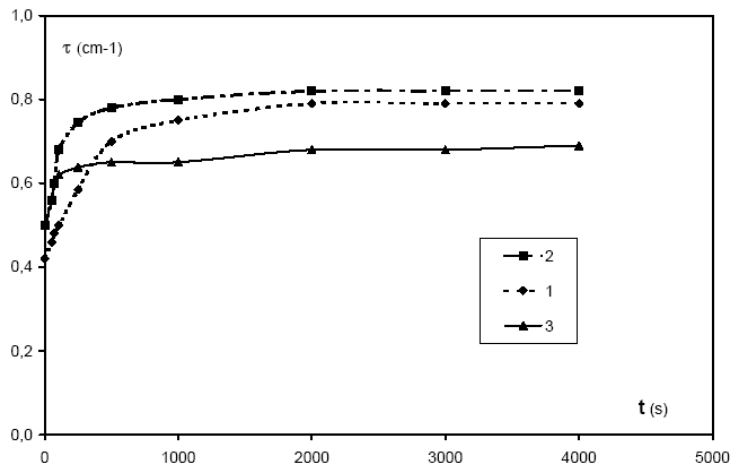
Figure 1. Influence of stirring rate on hydrophilic 0.5 μm silica aggregation. 1: 200 rpm; 2: 400 rpm; 3: 800 rpm
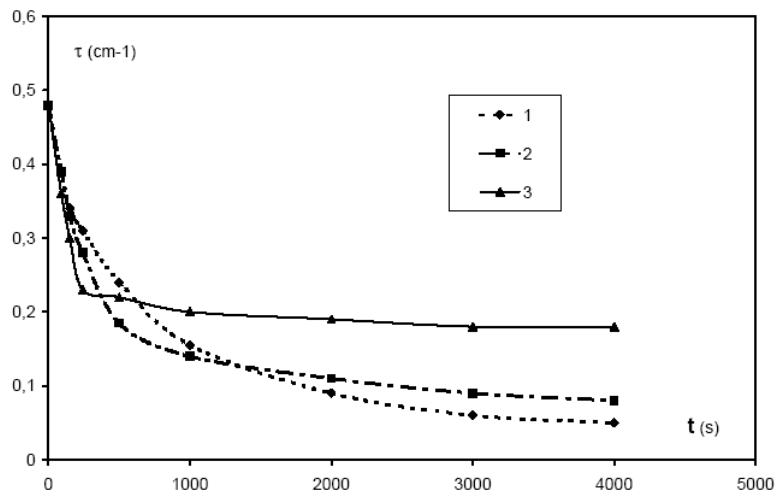

Figure 2. Influence of stirring rate on hydrophobic 0.5μm silica aggregation. 1: 200 rpm; 2: 400 rpm; 3: 800 rpm

Interpretation and Models

Aggregate morphology

Most recent experiments of aggregation in turbulent medium tend to prove that the aggregates have a fractal structure (Kusters et al., 1997; Gruy, 2001; Cugniet, 2003). An aggregate containing i identical primary particles of radius a_1 is characterised by its fractal dimension D_f and outer radius a_i which are linked by the relation:

$$a_i = a_1 \left(\frac{i}{Fs} \right)^{\frac{1}{Df}} \tag{3}$$

where Fs is a *structure factor*, which obeys the relation (Gmachowski, 1996):

$$Fs = 0.42D_f - 0.22 \tag{4}$$

According to the different authors, the fractal dimension corresponding to turbulent (local shear flow) aggregation is equal to 2.35 ± 0.15.

The fractal-like models are normally applicable only to large aggregates; Gruy (2001), however, has introduced the notion of *weak fractal dimension* (based on projected area of an aggregate on any plane) which can be extended to small aggregates and may make equations (3,4) suitable for them.

Aggregate optical properties

In a previous paper (Cournil et al., 2002), it was shown that hydrophobic particles are probably covered by a gas layer which invades their superficial porosity and that this gas layer may play an essential part both in the aggregate formation and fragmentation. In

8

particular, aggregate fragmentation is considerably reduced due to the presence of gas bridges between particles whereas effect of hydrophobicity is less noticeable on aggregation kinetics, i.e. the change of aggregate concentrations $N_i(t)$. As decrease in turbidity occurs as early as the start of aggregation, it is believed that new optical properties of the aggregates should be invoked at the first instance to explain the trend inversion in the turbidity variation. Sedimentation of large aggregates also occurs later on in the process.

Previous work on microbubbles-particles suspension

Suspensions with small particles and air bubbles (or microvoids) in a liquid or resin are met in the paints or coatings industry (Ross, 1971; Kerker et al., 1975). Generally a white paint film is composed of titania (TiO_2 , rutile) particles uniformly covered by a shell of silica, alumina or other materials. Opacity or hiding power is one of the main properties of a paint. It is due to multiple scattering of light by small particles. The higher the concentration of particles and the higher the optical contrast, the better the opacity. However, if the TiO_2 particle concentration is too large, particles can form aggregates, that are less efficient for scattering the light (Auger et al., 2003). In order to minimize the cost of white paint, one replaces rutile particles by small air bubbles, which are, however, less efficient scatterers than TiO_2 particles (Ross, 1971). So, a paint film can contain single rutile particles, microvoids or air microbubbles and aggregates of rutile particles. It has been suggested that the scattering efficiency could be improved by introducing rutile particles inside the microbubbles, due to the increased optical contrast (TiO_2 n = 2.8; air n = 1; resin n = 1.5). This situation is very similar to the system under study (SiO_2 n = 1.44; air n = 1; water n = 1.34).

Turbidimetry for diluted suspension rests on the "single scattering event" theory. For a monodisperse suspension, turbidity is expressed by:

$$\tau = l^{-1} = NC_{ext} = NC_{sca} \tag{5}$$

where l is the mean free path of photon. For a concentrated dispersion such as a paint, optical properties will be calculated in the framework of the radiative transfer theory. Simpler modelling of scattering in paints is also realized by using Kubelka-Munk theory (Ross, 1971). The main physical parameter for the two theories is the transport mean free path $l*$ defined as:

$$\left(l^*\right)^{-1} = N_{sca}\left(1 - \mu\right) = \phi S \tag{6}$$

with

$$S = \frac{1}{V_p} C_{sca}\left(1 - \mu\right) \tag{7}$$

where μ, ϕ, V_p are respectively the particle anisotropy factor, the volume fraction of particles and the volume of one particle. $l*$ and S characterize, respectively, the suspension and the particle. $l*^{-1}$ and S are also called the scattering efficiency of the film and of the particle. Kerker et al., (1975) studied a single titania particle coated by an air layer embedded in resin. They calculated its scattering efficiency as a function of the size parameter $v = 2\pi b / \lambda$ (b is the radius of the spherical particle - air layer set) and volume fraction ϕ_p of titania. When $v < 2$, the scattering efficiency presents a strong minimum for $0.2 < \phi_p < 0.5$ and the corresponding values of ϕ_p and S are dependent on v. This result was confirmed by Auger (Auger et al., 2004). A similar conclusion, by using C_{sca} / V_p as scattering efficiency, was

attained by Auger (Figs 4, 5, 6. in Auger et al., 2001) for $\nu < 10$. When $\nu \gg 2$, Kerker et al. (1975) observed a synergistic effect: the replacement of a part of the particle by a microvoid concentric spherical shell results in an enhancement of the scattering efficiency S (but, not for C_{sca} / V_p). This effect, though weaker, was confirmed by Auger et al.(2004) for $\nu > 5$. The transition value for ν between the two behaviours is dependent on the system: TiO$_2$ which is characterized by an high refractive index presents a maximum of scattering efficiency for a particle radius equal to about 0.2 µm ($1 < \nu = 2\pi a / \lambda < 2$). Then, minimum for scattering efficiency may occur for a spherical particle - air shell set, the size of which is larger than the one of a single particle having a maximal scattering efficiency. Kerker et al. (1975) suggested that the minimum of scattering efficiency can be explained in the framework of Rayleigh theory, i.e. by introducing the polarisability of a coated sphere (Kokhanovsky, 2001). Then, this is equivalent to the definition of an effective refractive index m_{cs} for small coated sphere:

$$\frac{(m_{cs}^2 - 1)}{(m_{cs}^2 + 2)} = \frac{(m'^2 - 1)(m^2 + 2m'^2) + \phi_p (m^2 - m'^2)(2m'^2 + 1)}{(m'^2 + 2)(m^2 + 2m'^2) + \phi_p (m^2 - m'^2)(2m'^2 - 2)} \tag{8}$$

m and m' are respectively the relative (compared to the continuous medium) refractive index of particle and gas. Minimum of scattering efficiency corresponds to this value of m_{cs}.

The displacement of the TiO$_2$ particle from the centre to the edge of the air bubble can lead to either an increase or a decrease of scattering cross section by a factor two (Auger et al., 2001). However, the effect of location of particle inside the air bubble on scattering properties is less pronounced than the effect of the particle location that can be inside or outside the air bubble (Fig 4. in Auger et al., 2001). This brief survey shows that the presence of microbubbles in suspension may lead to a decrease of its scattering properties.

To characterize the optical properties of silica suspensions, it is proposed to calculate

now the extinction cross section of the hydrophilic, then hydrophobic aggregates. Exact

methods could be used for calculating scattering properties of aggregates (see, for instance,

Xu, 1995; Xu, 1998; Auger et al., 2001; Auger et al., 2003). Due to time-consuming

computations, these calculations are restricted to very small aggregates and only used in the

case of simple aggregate morphology. As the aggregation process leads to a wide population

of aggregates with various morphologies, one needs approximate methods for extinction cross

section estimates.

Hydrophilic silica aggregates

Each aggregate is characterised by its radius a_i and its mean inner volume fraction $\bar{\phi}_a$

(deduced from (3)). Two kinds of modelling are successfully used to calculate optical

properties of small silica aggregates (Gruy, 2001).

- Effective Refractive Index method

The easiest way to determine the optical properties of an aggregate is to calculate its effective

refractive index m_a (see, for instance, Born and Wolf (1980); Vargas et al. (2000). The

equation derived by Maxwell-Garnett has been proved to be suitable (Gruy, 2001) for this

system:

$$\frac{(m_a^2 - 1)}{(m_a^2 + 2)} = \bar{\phi}_a \frac{(m^2 - 1)}{(m^2 + 2)}$$ (9)

m and m_a are the relative refractive indices respectively for primary particles and aggregates.

Given the radius and the effective refractive index of an aggregate, the Mie theory (van de

Hulst, 1957) can allow us to calculate the scattering cross section C_{sca} for a given wavelength

λ.

- Anomalous Diffraction method

Another simple way to calculate the optical properties of small silica aggregates considers interferences between electromagnetic waves scattered by each primary particle of the aggregate. In present case of 0.5 μm silica particles in water-ethanol solution, optical parameters have the following properties: $m-1 \langle\langle 1$ and $\frac{4\pi}{\lambda}a_1(m-1) \approx 1$. When $\frac{4\pi}{\lambda}a_1(m-1)$ is not too small, light scattering by particles follows the anomalous diffraction model (van de Hulst, 1957), i.e., globally, straight transmission and subsequent diffraction. In this case, scattered intensity is concentrated near the original direction of propagation and the extinction cross section is given by relation:

$$C_{ext} = 2\iint\limits_{S_p} (1 - \cos\frac{2\pi}{\lambda}\delta(m-1))dS_p \qquad (10)$$

Integration is performed over the object projected area S_p on a plane perpendicular to propagation direction. δ is the optical path length through the object. This calculated path is a function of the projection coordinates. As aggregate can randomly orientate, the optical properties are obtained after calculating an average over all orientations.

Hydrophobic silica aggregates

Refractive indices of silica, water and gases are respectively 1.44, 1.34 and 1.0. Scattering properties of particles in a medium mainly depend on the index contrast between the media and on the particle size. According to the works of Kerker et al. (1975) and Auger et al. (2001, 2004), presence of gas (air or vapour) in an aggregate may considerably change this

contrast and be responsible for the behaviour modification that was noted in Figures 1 and 2.

Calculation of the scattering properties of a silica-water-air aggregate requires assumptions on the three-phase (silica, water, gas) location. The two cases which have been envisaged - surrounding thin layer (Figure 3a) or homogeneous density in the porous particle (Figure 3b) (Cugniet, 2003) - give similar results.

In this paper, considered hydrophobic aggregates are a set of primary particles, each covered by a thin layer of gas. Then, one can apply the anomalous diffraction theory in order to calculate the extinction cross section:

$$C_{ext} = 2\iint_{S_p} \left[1 - \cos\left(\frac{2\pi}{\lambda} \left(\delta(m-1) + \delta'(m'-1) \right) \right) \right] dS_p \qquad (11)$$

δ and δ' are, respectively, the light path (function of the projection coordinates) through silica and gas. m and m' are, respectively, the relative refractive index of silica and gas. Figure 4 represents the ratio of scattering cross sections without and with gas versus gas content P (ratio of gas volume over silica volume) for different silica small aggregates ($D_f = 2.7$). One observes the decrease of scattering cross section with P whatever the aggregate size. This decrease is due to $m' < 1$ in equation (11).

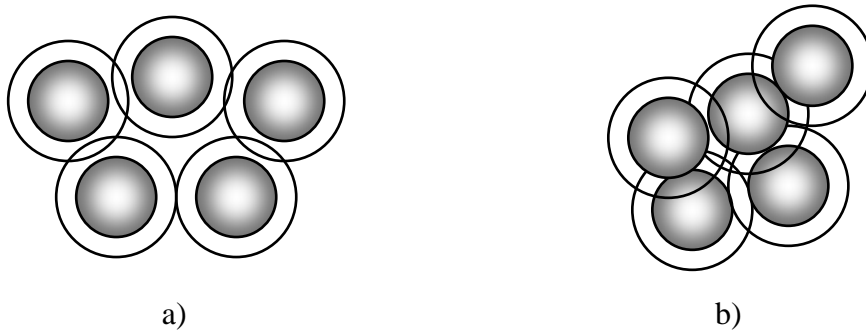a)   b)

Figure 3. Different gas-liquid-solid configurations in the hydrophobic aggregates: a) thin gas

layer located around each particle; b) homogeneous gas phase inside the aggregate

Because of time consuming calculations particularly for large aggregates by the previous method, a fast procedure resting on *Effective Refractive Index* method is proposed. It has been validated by comparison with numerical results coming from anomalous diffraction theory (equation 11). The approximated scattering cross section corresponds to a sphere (Mie theory) with equivalent radius $a_i^{'}$ (12a,12b,12c) and equivalent relative refractive index m_a' (13a,13b,13c) as follows:

$$a_i^{'} = a_1 \left(\frac{i}{Fs} \right)^{\frac{1}{D_f}} \left(1+P\right)^{\frac{1}{3}} \quad i > 2 \tag{12a}$$

$$a_1^{'} = a_1 \left(1+P\right)^{\frac{1}{3}} \tag{12b}$$

$$a_2^{'} = 1.364 a_1 \left(1+P\right)^{\frac{1}{3}} \tag{12c}$$

$$\frac{(m_a^{'2}-1)}{(m_a^{'2}+2)} = \frac{(m^2-1)}{(m^2+2)} \bar{\phi}_a A + \frac{(m^{'2}-1)}{(m^{'2}+2)} \left(P\bar{\phi}_a\right) B \tag{13a}$$

with
$$A = \bar{\phi}_a^{-\frac{0.3}{i}} \tag{13b}$$

and
$$B = b_1 e^{-b_2 \left(P\bar{\phi}_a\right)^2} \tag{13c}$$

Equation 12 takes into account the size change with the gas content. Equation 13 is a corrected Maxwell-Garnett expression: it contains two empirical parameters *A* and *B*. *A* is

only effective for very small aggregates ($i \leq 4$). In B expression, it appears two parameters b_1 and b_2 which are simple functions of D_f (Cugniet, 2003).

Another benefit of this procedure is that the effect of the turbidimeter acceptance angle can be easily taken into account in the framework of Mie theory for sphere (Gruy, 2001).
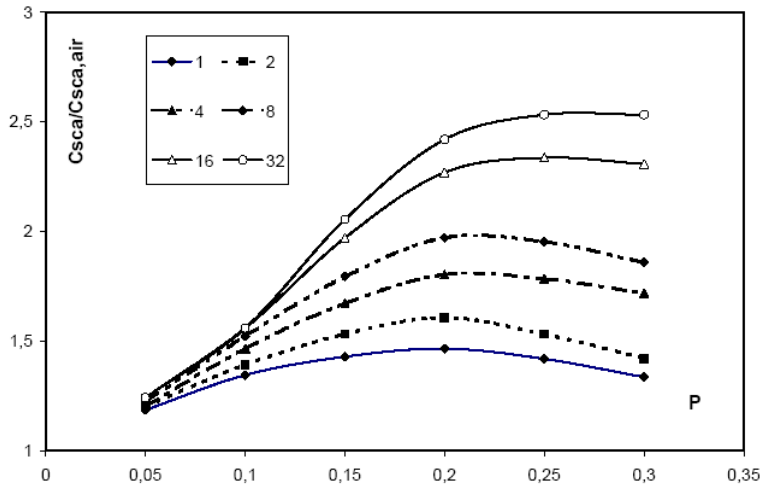

Figure 4. Ratio of scattering cross sections without and with gas versus gas content *P* for different silica aggregates (weak fractal dimension D_f = 2.7); primary particle number per aggregate is indicated on each plot

Simulations

Previous optical models can be used to calculate the turbidity of different suspensions of hydrophobic and hydrophilic silica aggregates. Given an aggregation model (Kusters et al. 1997), the variation with time of the aggregate population density can be calculated, thus the turbidity change over the aggregation process. By comparison between predicted and

measured turbidity plots versus time, the different models can be validated and the unknown parameters calculated.

This procedure was used recently in (Cugniet, 2003) to interpret the main aspects of hydrophilic and hydrophobic silica aggregation. We give here two typical examples of simulations. Figure 5 shows the experimental and simulated curves obtained for hydrophilic silica aggregation. Figure 6 relates to hydrophobic silica aggregation.
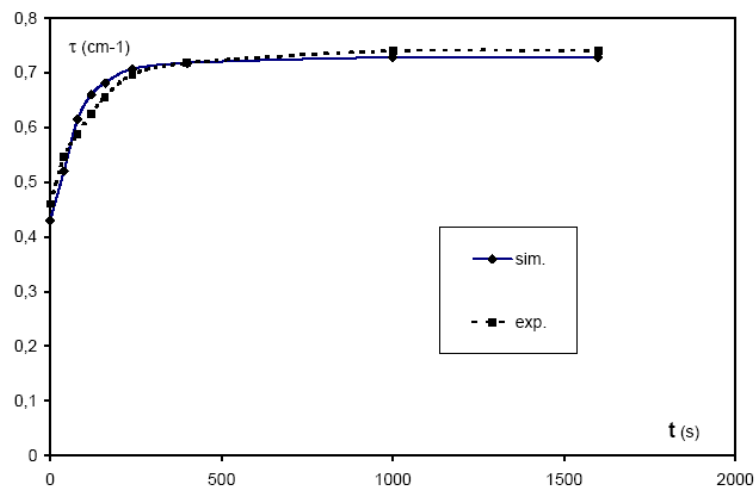

Figure 5. Comparison between experimental and simulated ($D_f = 2.4$; $L = 68$) turbidity plots for 0.5 μm hydrophilic silica particles aggregation at stirring rate 200 rpm.

Relevant simulation parameters are aggregate fractal dimension, respectively, 2.4 and 2.67 for hydrophilic and hydrophobic aggregates, and maximum particle number per aggregate, respectively, 68 and 2048 in this case. For hydrophobic aggregate, a volume fraction of 0.3 in gas corresponds to the best agreement between experimental and calculated curves.

From a strict optical point of view, this example confirms as well as many others (Cugniet, 2003) that the inversion in turbidity variation which was observed experimentally is due to the presence of gas in the hydrophobic silica aggregates.
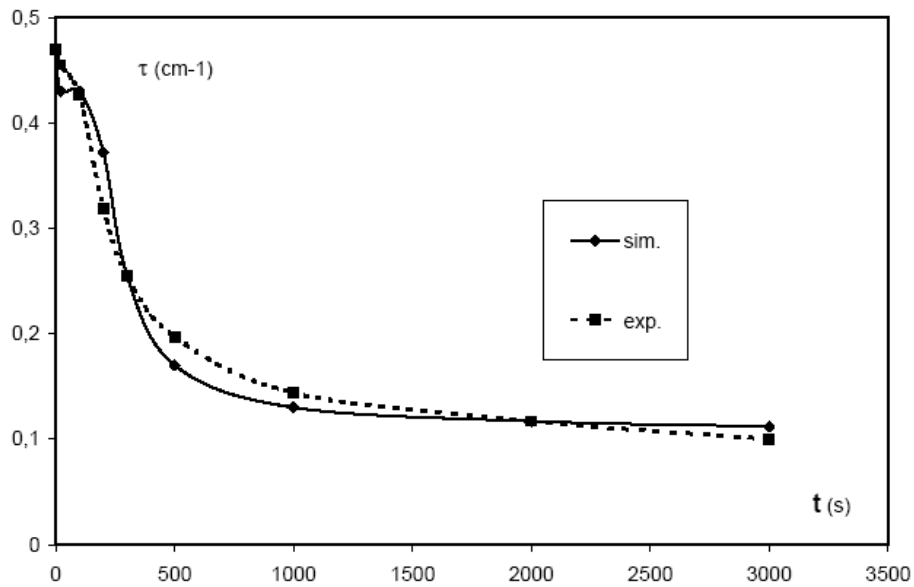

Figure 6. Aggregation of 0.5 μm hydrophobic silica at 200 rpm: experimental and simulated ($D_f = 2.67$; $L = 2048$; $P = 0.3$) turbidity curves.

Conclusion

The influence of stirring rate on aggregation of hydrophilic and hydrophobic silica in water was studied experimentally by turbidimetry. The strong differences in behaviour which are

clearly observed have an optical origin which expresses itself through modifications in the

structure of the aggregates. In addition to its interest relatively to original conditions of

aggregation, this paper presents new calculation procedures of light scattering cross-section of

small aggregates of micron sized silica particles in a liquid phase and of three-phase (gas-

liquid-solid) aggregates. The different models are validated using the available aggregation

experimental data.

References

Attard, P. 2003. Nanobubbles and the hydrophobic interaction. *Advanced Colloid and Interface Science* 104: 75- 91.

Auger, J.C., B. Stout, R.G. Barrera, F. Curiel 2001. Scattering properties of rutile pigments located eccentrically within microvoids. *J. of Quantitative Spectroscopy & Radiative Transfer* 70: 675-695.

Auger, J.C., R.G. Barrera, B. Stout 2003. Scattering efficiency of clusters composed by aggregated spheres. *J. of Quantitative Spectroscopy & Radiative Transfer* 79-80 : 521-531.

Auger, J.C., R.G. Barrera, B. Stout 2004. Optical properties of an eccentrically located pigment within an air bubble. *Progress in Organic Coatings* 49: 74-83.

Born, M. and E.Wolf 1980. *Principles of Optics* Oxford : Pergamon Press.

Cournil, M., F. Gruy, P. Gardin, H. Saint-Raymond 2002. Experimental study and modelling of inclusions aggregation in turbulent flows to improve steel cleanliness. *Physics State Solid (a)* 189: 159-168.

Crawley, G.M., M. Cournil, D. Di Benedetto. Size analysis of fine particle suspensions by spectral turbidimetry. *Powder Technology* 91:197-208.

Cugniet, P. 2003, PhD Dissertation, *Etude de l'agrégation de particules solides en milieu non mouillant* Ecole des Mines de Saint-Etienne (France).

Duchet, J., B. Chabert, J.P. Chapel, J.F. Gérard, J.M. Chovelon, N. Jaffrezic-Renault 1997. Influence of the deposition process on the structure of grafted alkysilane layers. *Langmuir* 13: 2271-2278.

Elimelech, M., J. Gregory, X. Jia, R. Williams 1995. *Particle Deposition & Aggregation* Oxford : Butterworth-Heinemann.

Gmachowski, L. 1996. Hydrodynamics of aggregated media. *Journal of Colloid and Interface Science* 178: 80-86.

Gruy, F. 2001. Formation of small silica aggregates by turbulent aggregation. *Journal of Colloid and Interface Science* 237: 28-39.

Gruy, F., M. Cournil, P. Cugniet 2004. Influence of non-wetting on the aggregation dynamics of micronic solid particles in turbulent medium *Journal of Colloid and Interface Science* in press.

Kerker, M., D.D. Cooke, W.D. Ross 1975. Pigmented microvoid coatings; Theooretical study of three models. *Paint Research Institute* 47: 33-42.

Kokhanovsky, A.A. 2001. *Optics of Light Scattering Media* 2nd Ed. Berlin: Springer-Praxis.

Kusters, K.A., J.G. Wijers J.G., Thoenes, D. 1997. Aggregation kinetics of small particles in agitated vessels. *Chem. Eng. Sci*. 52: 107-121.

Parker, J.L., P.M. Claesson, P. Attard 1994. Bubbles, cavities, and the long-ranged attraction between hydrophobic surfaces. *Journal of Physical Chemistry* 98: 8468- 8480.

Ross, W.D. 1971. Theoretical computation of light scattering power ; Comparison between TiO_2 and air bubbles. *J. of Paint Technology* 43: 50-66.

Saint-Raymond, H., F. Gruy, M. Cournil 1998. Turbulent aggregation of alumina in water and n-heptane. *Journal of Colloid and Interface Science* 202: 238-250.

van de Hulst, H.C. 1957. *Light Scattering by Small Particles* New York: Wiley.

Vargas, W.E., P. Greenwood, J.E. Otterstedt, G.A. Niklasson 2000. Light scattering in pigmented coatings: experiments and theory. *Solar Energy* 68: 553-561.

Xu, Y. 1995. Electromagnetic Scattering by an Aggregate of Spheres. *Appl. Opt*. 34/21: 4573-4588.

Xu, Y. 1998. Efficient Evaluation of Vector Translation Coefficients in multiparticle light scattering theories. *J. Comp. Phys.* 139: 137-165.

Yakubov, G.E., H.J. Butt, O.L. Vinogradova 2000. Interaction forces between hydrophobic surfaces. Attractive jump as an indication of formation of "stable" submicrocavities. *Journal of Physical Chemistry* 104: 3407-3410.

Yushchenko, V.S., V.V. Yaminsky, E.D. Shchukin 1983. Interaction between particles in a nonwetting liquid. *Journal of Colloid and Interface Science* 96: 307-314.